WATER RESOURCES RESEARCH, VOL. 37, NO. 2, PAGES 393–404, FEBRUARY 2001

Steady state mass transfer from single-component dense nonaqueous phase liquids in uniform flow fields

Tom C. Sale and David B. McWhorter

Department of Chemical and Bioresource Engineering, Colorado State University, Fort Collins

Abstract. In recent years it has become increasingly clear that most remedial technologies fail to completely remove dense nonaqueous phase liquid (DNAPL) from subsurface source zones. Recognition of this limitation leads to the question of what benefit can be achieved through partial removal of DNAPL. To address this issue, a mathematical technique referred to as the multiple analytical source superposition technique (MASST) has been developed. MASST is based on a conceptualization of a DNAPL source zone as a grouping of discrete subzones containing DNAPL (e.g., fingers and/or pools) separated by portions of the aquifer that are entirely free of DNAPL. Using analytical techniques, spatial superposition of responses to multiple sources is used to estimate aqueous mass transfer rates from individual subzones. This procedure accounts for multiple DNAPL subzones with different volumes, geometries, and locations within an overall source zone that is otherwise free of the nonaqueous liquid. The mass transfer rate from a particular subzone is affected by mass transfer from all other subzones in the vicinity. Groundwater flow is assumed to be uniform, and transport processes are considered to be at a steady state. Comparison of MASST results with exact analytical solutions and laboratory data confirms the validity of MASST. Sensitivity analyses indicate that source-zone architecture is a primary factor governing bulk mass transfer and source longevity. Analysis of rate-limited mass transfer within DNAPL subzones and advective-dispersive transport about DNAPL subzones indicates that advective-dispersive transport is the primary factor controlling mass transfer rates. Finally, results indicate that removal of the vast majority of the DNAPL will likely be necessary to achieve significant near-term improvements in groundwater quality.

1. Introduction

Typically, it is not possible to restore subsurface dense nonaqueous phase liquid (DNAPL) source zones so that they cease to affect exceedance of groundwater standards [*U.S. Environmental Protection Agency*, 1993]. Recognition of this fact has led to strategies that contain waters that would otherwise issue from the source zones. Containment of source zones reduces ongoing contributions to dissolved plumes. Common containment technologies include hydraulic containment, physical barriers, and reactive barriers.

The above approach notwithstanding, there remains significant pressure to remove mass from the source zone. If it is accepted that complete restoration of the source zone cannot be achieved, it is logical to inquire about the benefits that can be expected from removal of only a portion of the source-zone mass. A premise of our approach is that the benefits that may be derived from partial mass removal will be a consequence of reduced concentration in effluent from the "remediated" source zone. Reduced risk, source longevity, site-care requirements (e.g., monitoring), time of operation of plume control measures (e.g., pump and treat), and, perhaps, enhanced effectiveness of natural attenuation are among the potential benefits. All of these can be directly or indirectly linked to the concentration in waters leaving the source zone.

While these broad considerations motivate our research, it is clear that a key technical issue concerns the rate of mass transfer from the organic liquid to the aqueous phase. This paper presents a quantitative analysis of NAPL to water mass transfer in porous media. Through this, insights regarding governing processes are developed. Of course, mass transfer from NAPL to the aqueous phase is the subject of previous studies. A large portion of previous studies concerned the measurement of relevant mass-transfer-rate coefficients. The work presented herein focuses on the incorporation of available results into a computational scheme suitable for the practical estimation of three-dimensional mass transfer from multiple, discrete NAPL subzones. Our method is essentially analytical and therefore is well suited to handle the extreme spatial variation of solute concentration that occurs at various locations within an overall source zone composed of multiple, discrete NAPL subzones.

Paper number 2000WR900236.
0043-1397/01/2000WR900236$09.00

2. Conceptual Foundations

The primary focus of this research is chlorinated solvents in relatively uniform granular porous alluvium such as fluvial or eolian sand deposits. This focus notwithstanding, it is noted that much of the described work is applicable to other NAPLs in porous media and that the methods described herein have applicability in more complex hydrogeologic settings. The term source zone in this paper refers to the entire groundwater region in which DNAPL is present [*Feenstra et al.*, 1996]. The source zone is composed of multiple subzones in which the DNAPL resides. Subzones containing DNAPL are separated from one another by portions of the aquifer that are entirely

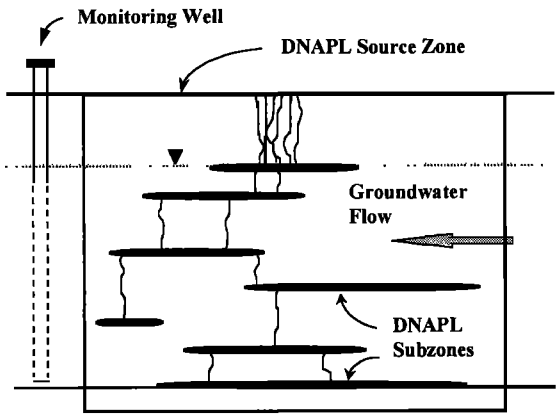

Figure 1. Conceptualization of a dense nonaqueous phase liquid (DNAPL) source zone.

free of DNAPL. Figure 1 is our version of the source-zone concept. This conceptualization is based upon laboratory studies [*Schwille*, 1988; *Kueper et al.*, 1989], limited field observations [*Poulson and Kueper*, 1992; *Kueper et al.*, 1993], and numerical simulations of DNAPL distributions in heterogeneous media [*Kueper and Frind*, 1991a, 1991b; *Kueper and Gerhard*, 1995]. Similar conceptualizations are presented by *Cohen and Mercer* [1993] and *Feenstra et al.* [1996].

Subzones containing DNAPL are distinguished by macroscopic boundaries within which the organic liquid may be continuous or at residual saturation. Because migration of DNAPL is highly sensitive to subtle, small-scale heterogeneity, it is expected that the distribution of DNAPL is complex within a particular source zone and highly variable from one source zone to another. Nevertheless, it is thought that DNAPL subzones often take the geometry of thin, horizontal lenses and pools, interconnected by vertical fingers that approximate the geometry of columns [*Anderson et al.*, 1992]. The term source-zone architecture is henceforth used to collectively refer to the number, dimensions, locations, and saturations of DNAPL subzones that compose the overall source zone.

The source-zone architecture formed by a particular DNAPL release depends upon the types of geologic units encountered by the DNAPL, the variability of the hydraulic and capillary properties of those units, the location and rates of release, and the properties of the DNAPL [*Kueper and Frind*, 1991a, 1991b]. It is expected that the flow of DNAPL slows following cessation of a release and a condition of mechanical equilibrium is approached. Interphase mass transfer occurs during DNAPL migration. Such transfer has no significant effect on the eventual source-zone architecture except, perhaps, in the case of DNAPL flow in small-aperture fractures bounded by porous matrix blocks into which components of the DNAPL diffuse [*Parker and McWhorter*, 1994; *Parker et al.*, 1996]. The primary effect of interphase mass transfer during active DNAPL migration is to establish local dissolved plumes around the still forming DNAPL subzones.

Once migration ceases, it is expected that a complicated distribution of dissolved DNAPL constituents has already evolved within the source zone. This distribution of dissolved chemicals frustrates the prescription of a realistic initial condition for the calculation of unsteady mass transfer once the DNAPL has ceased to migrate. Furthermore, the rates of dissolution reported by numerous authors [e.g., *Hunt et al.*, 1988; *Johnson and Pankow*, 1992; *Imhoff et al.*, 1994; *Voudrias and Yeh*, 1994; *Mayer and Miller*, 1996] suggest that source-zone architectures change very slowly once mechanical equilibrium is achieved. It is expected that instantaneous rates of mass transfer for particular source-zone architecture can be calculated as if the system were in a true steady state.

Interphase mass transfer, according to the single-resistance model, is expressed by [*Miller et al.*, 1990; *Powers et al.*, 1991; *Feenstra and Guiger*, 1996]

$$\dot{M}_v = K_L(C_s - C_a), \tag{1}$$

where $\dot{M}_v$ ($M\ T^{-1}\ L^{-3}$) is the rate at which mass is transferred from the DNAPL to the aqueous phase per unit volume of porous medium, C_s ($M\ L^{-3}$) is the effective aqueous solubility, and C_a is the bulk aqueous concentration. The mass transfer rate coefficient K_L ($1/T$) is an empirical parameter that is thought to be directly proportional to the molecular diffusion coefficient in the aqueous phase and the interfacial area between the two phases. Experimental determinations of the mass-transfer-rate coefficient are usually presented in the form of correlations involving the Sherwood, Schmidt, Peclet, and Reynolds numbers. Extensive presentation and discussion of such correlations are available in the literature [*Miller et al.*, 1990; *Powers et al.*, 1992, 1994; *Geller and Hunt*, 1993; *Imhoff et al.*, 1994; *Mayer and Miller*, 1996].

The rate of interphase mass transfer expressed by (1) is spatially variable within a subzone. Integration of (1) over the volume of the subzone calculates the total rate of interphase mass transfer attributable to the subzone. Considering a nonreactive contaminant and steady state conditions, the rate of interphase transfer must equal the rate at which dissolved mass is removed from the subzone by the processes of advection and mechanical dispersion. That is, the aqueous concentration within the subzone adjusts until the overall rate of interphase mass transfer is equal to the rate at which transport processes remove the dissolved substance from the subzone.

3. Multiple Analytical Source Superposition Technique (MASST)

The following describes a new mathematical method for estimating mass transfer rates from complex sets of single-component DNAPL subzones in uniform granular porous media. In general, the approach is analogous to the analytic element method for groundwater flow described by *Strack* [1989]. As a convenient shorthand, our method is referred to as MASST, for multiple analytical source superposition technique. Spatial superposition of analytically calculated responses to multiple sources is used to estimate aqueous mass transfer rates from individual subzones. Through this procedure, MASST accounts for multiple DNAPL subzones with different volumes, geometries, and locations within an overall source zone that is otherwise free of the nonaqueous liquid. Mass transfer from all other subzones in the vicinity affects the mass transfer rate from a particular subzone, and such potential interferences are given full consideration in MASST.

3.1. General Assumptions

Equation (2) presents a general form of the governing equation for three-dimensional transport of an aqueous phase solute in a uniform flow field in porous media:

$$\frac{\partial(V_w C_a)}{\partial x} - \frac{\partial}{\partial x}\left(D_x \frac{\partial C}{\partial x}\right) - \frac{\partial}{\partial y}\left(D_y \frac{\partial C}{\partial y}\right) - \frac{\partial}{\partial z}\left(D \frac{\partial C}{\partial z}\right) - \frac{\dot{M}_v}{\phi} - \frac{\dot{G}_v}{\phi} = -\frac{\partial C_a}{\partial t}. \quad (2)$$

The coordinate system employed in (2), and in all subsequent discussions, is the usual orthogonal Cartesian system with x positive in the direction of groundwater flow. The horizontal and vertical coordinates are y and z, respectively. $\dot{M}_v$ is the rate of mass transfer per unit volume of porous medium associated with either sorbed constituents or DNAPL ($M\ T^{-1}\ L^{-3}$). $\dot{G}_v$ is the rate of mass loss or addition due to reactions ($M\ T^{-1}\ L^{-3}$). Variables D_x, D_y, and D_z are dispersion coefficient ($L^2\ T^{-1}$) in the x, y, and z directions, respectively, V_w ($L\ T^{-1}$) is the seepage velocity, t (T) is time, and ϕ is porosity.

Simplification of (2) is achieved with the following assumptions: (1) Seepage velocity, transverse dispersion, and longitudinal dispersion are constants, (2) solutes of concern are nonreactive, (3) the dispersion coefficients D_y and D_z are equal and defined as D_T, the transverse dispersion coefficient ($L^2\ T^{-1}$), and (4) for consistency D_x is redefined as D_L, the longitudinal dispersion coefficient ($L^2\ T^{-1}$). These simplifications result in

$$\frac{D_L \partial^2 C_a}{\partial x^2} + \frac{D_T \partial^2 C_a}{\partial y^2} + \frac{D_T \partial^2 C_a}{\partial z^2} + \frac{\dot{M}_v}{\phi} - \frac{V_w \partial C_a}{\partial x} = \frac{\partial C_a}{\partial t}. \quad (3)$$

3.2. Aqueous Concentrations About a Discrete Subzone Source

Following *Hunt* [1960], a solution for (3) can be obtained wherein $\dot{M}_v$ occurs only within a discrete portion of the solution domain. This begins by considering the instantaneous point source solution

$$C_a(x, y, z, t) = \frac{M \exp\left(-\dfrac{((x - x_i) - V_w t)^2}{4D_L t} - \dfrac{(y - y_i)^2 + (z - z_i)^2}{4D_T t}\right)}{8\phi\sqrt{\pi^3 t^3 D_T D_L^2}}, \quad (4)$$

where M is a mass instantaneously introduced at the point with coordinates (x_i, y_i, z_i). Integration of (4) over a right parallelepiped subzone of DNAPL yields

$$C_a(x, y, z, t) = \int_{-a}^{a}\int_{-b}^{b}\int_{-c}^{c}\left[M_v \exp\left(-\frac{((x - (x_i - x')) - V_w t)^2}{4D_L t} - \frac{(y - (y_i - y'))^2 + (z - (z_i - z'))^2}{4D_T t}\right)\right] \cdot (8\phi\sqrt{\pi^3 t^3 D_T D_L^2})^{-1}\, dz'\, dy'\, dx', \quad (5)$$

where a, b, c are the half length, width, and height of the subzone as shown in Figure 2. M_v is the mass per unit volume instantaneously and uniformly transferred from the DNAPL into the aqueous phase within the subzone ($M\ L^{-3}$). As written in (5), the coordinate x_i, y_i, z_i is the geometric center of the source zone.

The integration indicated in (5) yields

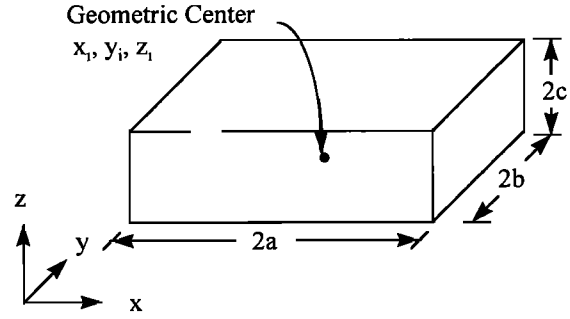

Figure 2. Conceptualization of a DNAPL subzone as a right parallelepiped.

$$C_a(x, y, z, t) = \frac{M_v}{\phi} f_x(x, t) f_y(y, t) f_z(z, t), \quad (6)$$

where

$$f_x(x, t) = \frac{1}{2}\left(\operatorname{erf}\left(\frac{x - x_i + a - V_w t}{\sqrt{4D_L t}}\right) - \operatorname{erf}\left(\frac{x - x_i - a - V_w t}{\sqrt{4D_L t}}\right)\right) \quad (7)$$

$$f_y(y, t) = \frac{1}{2}\left(\operatorname{erf}\left(\frac{y - y_i + b}{\sqrt{4D_T t}}\right) - \operatorname{erf}\left(\frac{y - y_i - b}{\sqrt{4D_T t}}\right)\right) \quad (8)$$

$$f_z(z, t) = \frac{1}{2}\left(\operatorname{erf}\left(\frac{z - z_i + c}{\sqrt{4D_T t}}\right) - \operatorname{erf}\left(\frac{z - z_i - c}{\sqrt{4D_T t}}\right)\right). \quad (9)$$

The solution for steady transport from a right parallelepiped source zone is obtained by integrating (6) with respect to time from 0 to ∞. This results in

$$C_a(x, y, z) = \frac{\dot{M}_v}{\phi}\int_0^\infty f_x(x - x_i, t) f_y(y - y_i, t) f_z(z - z_i, t)\, dt. \quad (10)$$

As a point of departure from *Hunt* [1960], substitution of (1) for $\dot{M}_v$ results in

$$C_a(x, y, z) = \frac{K_l(C_s - C_a(x_i, y_i, z_i))}{\phi} \cdot \int_0^\infty f_x(x - x_i, t) f_y(y - y_i, t) f_z(z - z_i, t)\, dt. \quad (11)$$

Equation (11) calculates the concentration due to steady rate-limited mass transfer from a subzone in the form of a right parallelepiped with center at (x_i, y_i, z_i). From this point forward the subzone is assumed to contain DNAPL and is referred to as a DNAPL subzone. The general point (x, y, z) may be located anywhere in the solution space, including the interior of the DNAPL subzone. A primary assumption used in developing (11) is that K_l and C_a are constants within the individual DNAPL subzone described by (x_i, y_i, z_i) and the dimensions a, b, and c. Where spatial variation of K_l and C_a is a concern, multiple subzones can be placed adjacent to one another to approximate a larger DNAPL zone. Strictly, the assumptions of constant K_l and C_a in an individual subzone are only true as the volume of the subzone approaches zero.

The sensitivity of MASST solutions to the number of subzones used to define field-scale DNAPL zones is addressed in subsequent sections.

3.3. Mass Transfer From a Single DNAPL Subzone

The rate of mass transfer from a single DNAPL subzone is obtained by evaluating (11) at (x_i, y_i, z_i), solving for $C_a(x_i, y_i, z_i)$, and substituting the result into (1). This yields (12) and (13) with the function F_o (units of time) defined in (14).

$$C_a(x_i, y_i, z_i) = C_s F_o \Big/ \left(\frac{1}{K_l} + F_o\right) \tag{12}$$

$$\dot{M}_v = C_s \Big/ \left(\frac{1}{K_l} + F_o\right) \tag{13}$$

$$F_o = \frac{1}{\phi} \int_0^\infty f_x(0, t) f_y(0, t) f_z(0, t)\, dt. \tag{14}$$

An interesting aspect of (13) is that it can be used to evaluate the relative significance of so-called "rate-limited mass transfer" characterized by K_l and spatial transport constraints about the DNAPL subzone characterized by F_o. For all but very small DNAPL subzones and large seepage velocities, the denominator of (12) and (13) is dominated by F_o. As an example, considering $a = 0.10$ m, $b = 0.10$ m, $c = 0.01$ m, $V_w = 0.1$ m d^{-1}, $\phi = 0.3$, $D_L = 10^{-6}$ m^2 s^{-1}, and $D_T = 10^{-8}$ m^2 s^{-1}, the value of F_o is 5.6 days. This is far larger than reported values of $1/K_l$ that fall in the range of 0.01–0.001 day [*Miller et al.*, 1990; *Imhoff et al.*, 1994]. The dominance of F_o in the denominator indicates that the concentration within a DNAPL subzone, with dimension greater than a few centimeters, must be very close to effective solubility. This condition has been widely documented in laboratory studies [e.g., *Miller et al.*, 1990; *Powers et al.*, 1994; *Imhoff et al.*, 1994]. These observations suggest that mass transfer from field-scale DNAPL zones is not strongly constrained by rate-limited mass transfer as prescribed by K_l. Further consideration of this topic is provided in the subsequent discussion of interphase mass transfer at a macroscopic scale.

3.4. Superposition of Multiple Analytical Sources

Mass transfer rates from multiple DNAPL subzones or from subdivisions of a single subzone can be estimated through spatial superposition of responses to multiple sources. Again, this procedure is referred to as the multiple analytical source superposition technique, or MASST. As shown in (15), MASST involves development of an equation that describes the concentration at the geometric center of the jth subzone (x_j, y_j, z_j) as the result of steady state mass transfer from N subzones.

$$C_a(x_j, y_j, z_j) = \sum_{i=1}^{N} K_l(C_s - C_a(x_i, y_i, z_i)) \cdot F(x_j - x_i, y_j - y_i, z_j - z_i) \qquad i, j = 1, 2, 3, \ldots, N. \tag{15}$$

Equation (15) represents a set of N equations with N unknown concentrations at the geometric center of each subzone. Solving this set of equations for the concentration at the geometric centers of the subzones results in the matrix equation

$$\mathbf{C}_a = C_s([F] + K_l^{-1}[I])^{-1}[F]\mathbf{U}, \tag{16}$$

where $\mathbf{C}_a$ is an N component vector of concentrations at the geometric centers of the subzones, $[F]$ is an N by N matrix of transport constraint functions, $[I]$ is an N by N identity matrix, and $\mathbf{U}$ is an N component vector of unit values (the unity vector). Substitution of $\mathbf{C}_a$ into (1) yields

$$\dot{\mathbf{M}}_v = C_s([F] + K_l^{-1}[I])^{-1}\mathbf{U}, \tag{17}$$

where $\dot{\mathbf{M}}_v$ ($M\ T^{-1}\ L^{-3}$) is an N component vector of mass transfer rates per unit volume from the N individual subzones. It will be noted that (17) is the multisubzone equivalent of (13). Finally, the total rate of mass transfer ($M\ T^{-1}$) from the set of N subzones is

$$\dot{M}_T = \sum_{i=1}^{N} \dot{M}_{v_i} V_{s_i}, \tag{18}$$

where V_{s_i} is the bulk volume of the ith subzone. Equations (16)–(18) are the core equations used throughout the remainder of this paper.

4. Confirmation of MASST

The following presents comparisons of MASST results with exact analytical solutions for simple cases where such solutions are possible. Through this process it is shown that MASST provides accurate solutions to the governing equations. In addition, MASST solutions are fit to laboratory measurements of mass transfer. This effort shows that close agreement is obtained using "typical" transport parameters and further supports the validity of MASST.

The first problem considered is mass transfer inside a uniform DNAPL zone that begins at $x = 0$. This is analogous to dissolution in an infinite column containing a uniform porous medium with uniform DNAPL saturation. The second problem is mass transfer from a uniform plane source that begins at $x = 0$. All calculations were performed using a 120-MHz Pentium personal computer and MATHCAD 7.0 [*MathSoft, Inc.*, 1997]. Numerical integrations were carried out using a Romberg integration scheme. This integration scheme is a standard component of MATHCAD 7.0.

4.1. Transport Inside a Uniform DNAPL Zone

Assumptions of steady state nonreactive transport in a uniform DNAPL zone beginning at $x = 0$ results in the following governing equation and boundary conditions:

$$\frac{D_L \partial^2 C_a}{\partial^2 x} - \frac{K_l(C_s - C_a)}{\phi} = \frac{V_w \partial C_a}{\partial x} \tag{19}$$

$$V_w C_a = D_L \frac{dC_a}{dx} \qquad x = 0 \tag{20}$$

$$\frac{dC_a}{dx} = 0 \qquad x = \infty. \tag{21}$$

Note the boundary condition introduced in (20) is different from the zero concentration at $x = 0$ condition used by *Miller et al.* [1990] for the same problem. The condition expressed by (20) is a flux-type boundary condition and takes into account the fact that diffusion can transport contaminants into the influent aqueous phase. Following *van Genuchten and Alves* [1982], a solution for C_a is obtained. Substitution of this solution into the expression for rate of mass transfer (1) yields

$$\dot{M}_v = C_s K_l \frac{2}{1 + (1 + (4K_l D_L / V_w^2 \phi))^{1/2}} \cdot \exp\left(\frac{V_w x}{2D_L}\left(1 - \left(1 + \frac{4K_l D_L}{V_w^2 \phi}\right)^{1/2}\right)\right). \quad (22)$$

Application of MASST to this one-dimensional transport problem is achieved by setting b and c equal to ∞ in (8) and (9). This causes both (8) and (9) to equal unity and the transport function to become

$$F = \frac{1}{\phi}\int_0^\infty f_x(x, t)\, dt. \quad (23)$$

MASST estimates of mass transfer are obtained by approximating the DNAPL zone as a sequence of subzone layers (infinite in the x and z dimensions) to which (17) and (18) are applied with F given by (23). Conditions considered are $V_w = 1 \times 10^{-5}$ m s^{-1}, $D_L = 1 \times 10^{-6}$ m^2 s^{-1}, $\phi = 0.3$, $C_s = 1000$ mg L^{-1}, and $K_l = 100$ day^{-1}. Figure 3 compares MASST estimates with results obtained using the exact analytical solution (22). The MASST solution is based on 18 continuous subdivisions of a total length of 0.05 m. The length of the individual subzones ($2a_i$) was selected so that total mass transfer was approximately the same in each of the subzones. This was done to accommodate the assumption of uniform C_a and K_L throughout each subzone. Further improvement in accuracy can be achieved by increasing the number of subzones. The close fit observed in Figure 3 indicates that MASST provides a reasonable approximation to the exact solution to (19) subject to (20) and (21).

Further confidence in MASST can be achieved by considering laboratory column data. Using data from *Miller et al.* [1990], Figure 4 presents rates of toluene dissolution as a function of seepage velocity. Figure 4 also presents MASST estimates based on one-dimensional transport with rate-limited mass transfer. Following *Bear* [1972], estimates of D_L were obtained using

$$D_L = D_e + \alpha_L V_w. \quad (24)$$

The effective diffusion coefficient (D_e) and longitudinal dispersivity (α_L) were assumed to be 7×10^{-10} m^2 s^{-1} and 1×10^{-2} m, respectively. MASST was fit to the laboratory data using a K_l value of 360 day^{-1}. The close fit using typical laboratory scale values for α_L and K_l provides further confirmation of MASST.

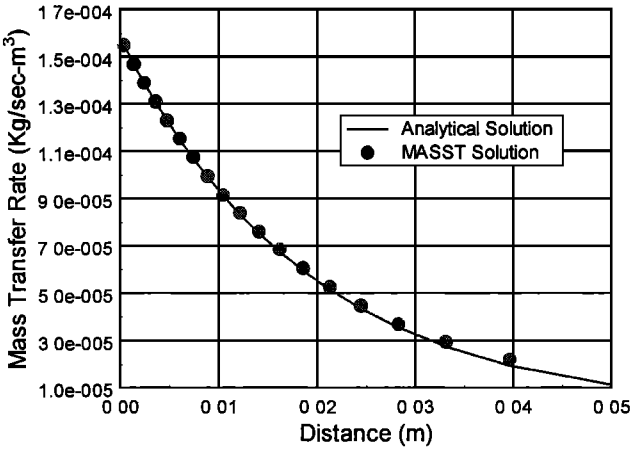

Figure 3. Comparison of multiple analytical source superposition technique (MASST) results with an exact analytical solution for mass transfer as a function of distance along a homogeneous column containing DNAPL.

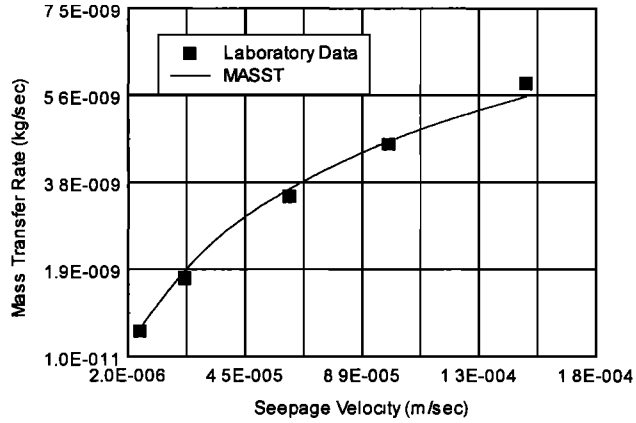

Figure 4. MASST fit to measured mass transfer rates in a laboratory column as a function of seepage velocity [*Miller et al.*, 1990].

4.2. Plane Source of Constant Concentration

Assuming that longitudinal dispersion is negligible relative to longitudinal advection, the governing equation for steady two-dimensional transport with one-dimensional flow is

$$V_w \frac{dC_a}{dx} = D_T \frac{d^2 C_a}{dz^2}. \quad (25)$$

Relevant boundary conditions for a semi-infinite plane of constant concentration located at $x \geq 0$ and $z = 0$ are

$$C_a = C_s \qquad x > 0, z = 0 \quad (26)$$

$$C_a = 0 \qquad x = 0 \quad (27)$$

$$C_a = 0 \qquad z = \infty. \quad (28)$$

As described by *Bird et al.* [1960], *Hunt et al.* [1988], and *Johnson and Pankow* [1992], the solution to (25) subject to (26), (27), and (28) is

$$C_a(x, z) = C_s\left(1 - \text{erf}\left(\frac{z}{2\sqrt{D_T x / V_w}}\right)\right), \quad (29)$$

and the mass flux from the plane source as a function of distance along the pool is

$$J(x) = C\phi\sqrt{V_w D_T / x\pi}. \quad (30)$$

The corresponding MASST solution is obtained by employing an infinite K_l value to achieve the condition of $C_a = C_s$ for $x \geq 0$ and $z = 0$. This allows simplification of (17) to

$$\dot{\mathbf{M}}_v = C_s[F]^{-1}\mathbf{U} \quad (31)$$

Furthermore, assuming $b = \infty$ and $z = 0$,

$$F_{i,j} = \frac{1}{2\pi\phi\sqrt{D_T D_L}}\int_{x_i - x_j - a}^{x_i - x_j + a} \exp\left(\frac{V_w u}{2D_L}\right) K_0\left(\frac{V_w u}{2D_L}\right) du, \quad (32)$$

where K_0 is the modified, zero-order Bessel function of the second kind and $i, j = 1, 2, \ldots, N$. Equation (32) was

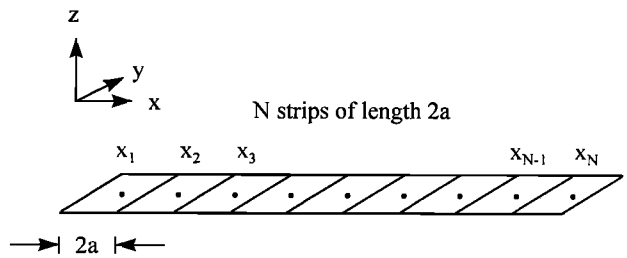

Figure 5. Concept of a segmented plane source.

obtained by integrating the closed-form solution for an infinite steady line source [*Hunt*, 1960] along the length of the pool. Limits of integration describe the distances between the center of the individual plane source of interest x_i and all other plane sources located at x_j. The concept of a segmented plane source is presented in Figure 5.

Figure 6 compares estimates of the mass transfer rates per unit area of plane source developed using the exact analytical solution (30) and the MASST solution presented in (31). Conditions considered are $V_w = 1 \times 10^{-5}$ m s^{-1}, $D_T = 1 \times 10^{-9}$ m^2 s^{-1}, $\phi = 0.3$, $C_s = 1000$ mg L^{-1}, and $D_L = 1 \times 10^{-8}$ m^2 s^{-1}. Since D_L is absent in (39), a small value of D_L was employed in (40) such that a direct comparison between the exact analytical and MASST solutions can be made. Overall, the sensitivity to D_L is small. This is because longitudinal dispersion is negligible relative to longitudinal advection for the conditions considered.

MASST calculations were made by subdividing a plane source, 0.1 m in length and infinitely wide, into 30 strips of equal length. As with the column solution, subdividing the source improves the accuracy of the MASST solution due to a closer approximation to the condition of a uniform K_l and C_a along each strip used to approximate the plane source.

It is important to note that the total mass transfer rate is proportional to the area beneath the two data sets in Figure 6. Thus the two solutions estimate nearly identical rates of total mass transfer. Experience with MASST indicates that local errors in estimated mass transfer rates, associated with too few subdivisions, tend to balance each other out. In the extreme case of approximating the plane with a single subdivision, MASST underestimates the total mass transfer rate by approximately 10%. The close agreement between the exact analytical and MASST solutions confirms that MASST also provides an accurate solution to (25) subject to (26), (26), and (28). Similar results are observed for the range of plausible input parameters.

Again, further confidence in MASST can be developed through consideration of laboratory data. *Schwille* [1988] reports laboratory measurements of mass transfer from a DNAPL pool as a function of seepage velocity. The experiment involved a pool of trichoroethene 1 m in length (x dimension) and 0.5 m in width (y dimension). Figure 7 presents measured mass transfer rates and MASST estimates as a function of seepage velocity. MASST estimates were developed using (31) and (32). The dispersion coefficients D_L and D_T were estimated using (24) with α_L and α_T values of 0.01 and 0.0002 m, respectively. Through variation of α_L and α_T, it was observed that the MASST estimates were largely insensitive to α_L, and consequently, the true fitting parameter was α_T. Again, close agreement between measured mass transfer rates and MASST estimates supports the validity of MASST.

5. Dimensionless Form of MASST

Dimensionless forms of MASST are developed by casting (16) through (18) in terms of dimensionless variables. This allows for a more direct analysis of factors affecting mass transfer. As a first step, all length variables are divided by a macroscopic length, taken to be the length of a DNAPL subzone (L), measured in the direction of aqueous flow. Macroscopic Sherwood and Peclet numbers are defined as

$$Sh_m = \frac{K_l L^2}{D_L \phi} \tag{33}$$

$$Pe_m = \frac{V_w L}{D_L}. \tag{34}$$

Both the Sherwood and Peclet numbers are subscripted with m to emphasize that they are macroscopic parameters that should not be confused with pore-scale Sherwood and Peclet numbers that have appeared in the literature [*Miller et al.*, 1990; *Parker et al.*, 1991; *Powers et al.*, 1992; *Geller and Hunt*, 1993; *Imhoff et al.*, 1994; *Powers et al.*, 1994]. Further simplification is achieved by defining

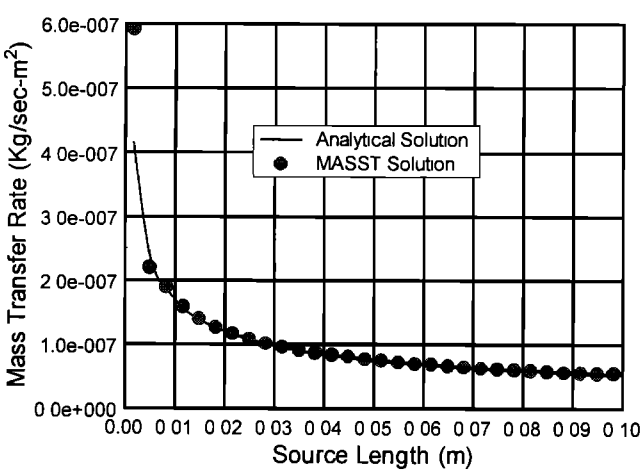

Figure 6. Comparison of MASST results with an exact analytical solution for mass transfer rate as a function of position along a plane source of constant concentration.

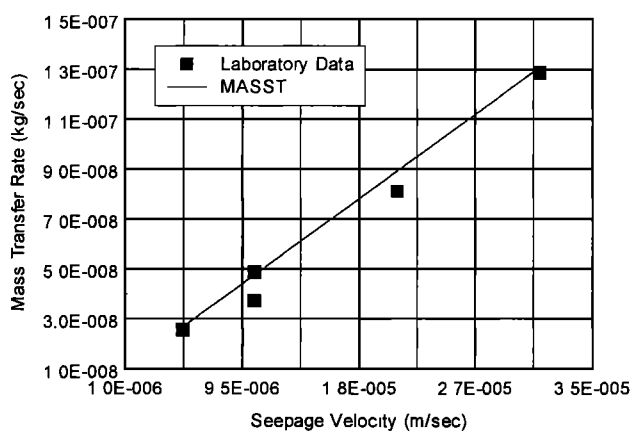

Figure 7. MASST fit to measured laboratory pool mass transfer rates as a function of seepage velocity [*Schwille*, 1988].

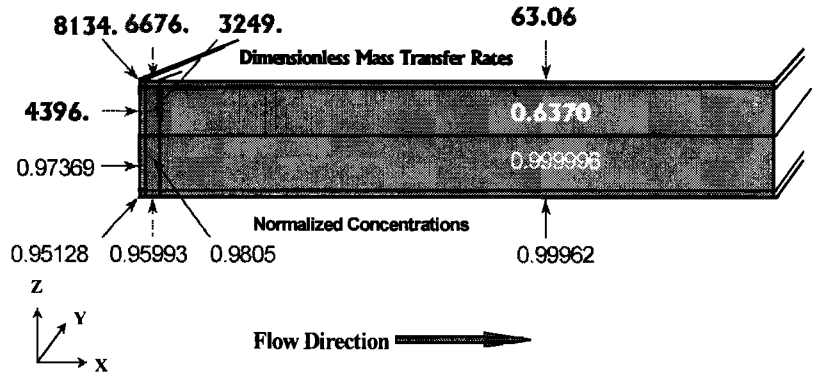

Figure 8. Dimensionless mass transfer rates and normalized concentrations within a DNAPL subzone.

$$D_r = \frac{D_L}{D_T} \tag{35}$$

$$T = \frac{tD_L}{L^2} \tag{36}$$

$$C_{na} = \frac{C_a}{C_s}. \tag{37}$$

With the above definitions of dimensionless parameters and variables, the dimensionless form of the transport matrix is

$$F_{d_{i,j}} = \frac{1}{\phi}\int_0^\infty f_{dx}(X_j - X_i, T) f_{dy}(Y_j - Y_i, T) f_{dz}(Z_j - Z_i, T)\, dT, \tag{38}$$

where

$$f_{dx}(X_j - X_i, T) = \frac{1}{2}\left(\operatorname{erf}\left(\frac{X_j - X_i + A - Pe_m T}{\sqrt{4T}}\right) - \operatorname{erf}\left(\frac{X_j - X_i - A - Pe_m T}{\sqrt{4T}}\right)\right) \tag{39}$$

$$f_{dy}(Y_j - Y_i, T) = \frac{1}{2}\left(\operatorname{erf}\left(\frac{Y_j - Y_i + B}{\sqrt{4T}}\right) - \operatorname{erf}\left(\frac{Y_j - Y_i - B}{\sqrt{4T}}\right)\right) \tag{40}$$

$$f_{dz}(Z_j - Z_i, T) = \frac{1}{2}\left(\operatorname{erf}\left(\frac{Z_j - Z_i + C}{\sqrt{4T}}\right) - \operatorname{erf}\left(\frac{Z_j - Z_i - C}{\sqrt{4T}}\right)\right). \tag{41}$$

Note the quantities A, B, C, X, Y, and Z are all equal to the dimensional lowercase equivalents divided by the subzone length L.

Finally, the dimensionless equivalents of (16), (17), and (18) are

$$\mathbf{C_{na}} = ([F_d] + Sh_m^{-1}[\mathbf{I}])^{-1}[F_d]\mathbf{U} \tag{42}$$

$$\dot{\mathbf{M}}_{vd} = ([F_d] + Sh_m^{-1}[\mathbf{I}])^{-1}\mathbf{U} \tag{43}$$

$$\dot{M}_{Td} = \sum_{i=1}^{N} V_{d_i} M_{vd_i}, \tag{44}$$

where $\mathbf{C_{na}}$ is an N component vector of normalized concentrations at the geometric center of the subzones, V_{d_i} is the volume of the ith DNAPL subzone, $\dot{\mathbf{M}}_{vd}$ is a vector of dimensionless mass transfer rates per unit volume, and $\dot{M}_{Td}$ is the dimensionless total mass transfer rate for the subzone. Definitions of $\dot{\mathbf{M}}_{vd}$ and $\dot{M}_{Td}$ in terms of dimensional quantities are presented in (45) and (46).

$$\dot{\mathbf{M}}_{vd} = \frac{\dot{\mathbf{M}}_v L^2}{D_L C_s \phi} \tag{45}$$

$$\dot{M}_{Td} = \frac{\dot{M}_T}{D_L C_s L \phi}. \tag{46}$$

Derivation of (38) through (44) is presented by *Sale* [1998].

6. Mass Transfer as a Function of Position Within a DNAPL Subzone

The following presents an analysis of mass transfer rates within a single subdivided DNAPL subzone. This is accomplished using the dimensionless form of MASST to calculate normalized concentrations and dimensionless mass transfer rates through a cross section of a DNAPL subzone. Figure 8 presents a cross section of a DNAPL subzone cut parallel to the flow direction. The subzone has dimensionless lengths of $X = 1$, $Y = \infty$, and $Z = 0.1$. Assumed dimensionless transport inputs are $Sh_m = 1 \times 10^5$, $Pe_m = 10$, and $D_r = 100$. Selection of these values reflects typical conditions defined by $\alpha_L = 0.1$ m, $\alpha_T = 0.001$ m, $K_L = 500$ day^{-1}, $L = 1$ m, and $V_w = 0.1$ m d^{-1}. Also shown in Figure 8 are subzone subdivisions of dimensionless length 0.001, 0.0017, and 0.9973 in the X dimension and 0.005, 0.045, 0.045, and 0.005 in the Z dimension (see lines within the subzone). This subdivision of the subzone results in similar rates of total mass transfer within each subdivision.

Calculated dimensionless mass transfer rates per unit volume ($\dot{M}_{vd}$) and normalized concentrations (C_{na}) are shown in the upper and lower mirror halves of the subzone, respectively. The values posted were calculated using (42) and (43). An important observation drawn from the data is that the highest rates of mass transfer occur at the leading edges of the subzone. Moving from the leading edge of the subzone at the upper left-hand corner to the trailing edge at the right-hand corner, $\dot{M}_{vd}$ decreases by 2 orders of magnitude. Similarly, moving from the leading edge of the subzone in the upper left-hand corner to the interior 90% of the subzone (represented by the two largest subdivisions), $\dot{M}_{vd}$ decreases by 4

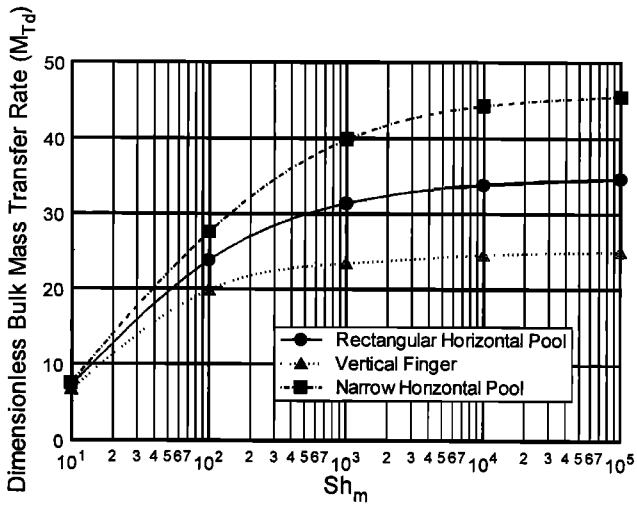

Figure 9. Sensitivity of dimensionless mass transfer rates to the modified Sherwood number.

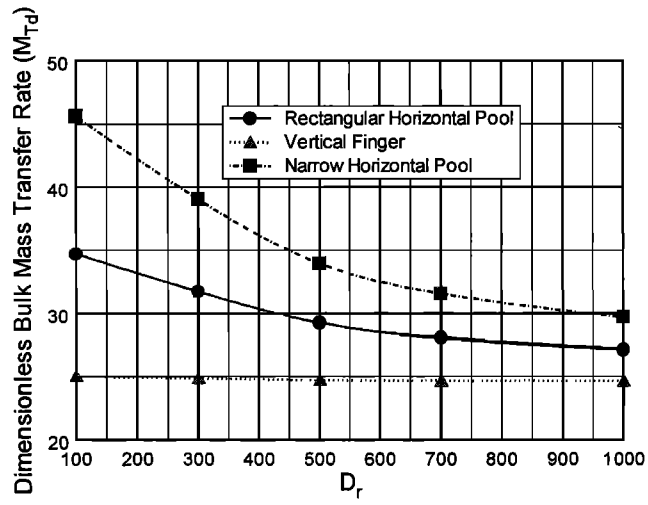

Figure 11. Sensitivity of dimensionless mass transfer to the ratio of longitudinal and transverse hydrodynamic dispersion.

orders of magnitude. Normalized concentration values show the same trend. The normalized difference in chemical potential that drives transfer ($1 - C_{na}$) ranges from 0.049 at the leading corners of the subzone to 0.000004 within the interior of the subzone. In all cases, normalized concentration is close to 1. This suggests that the overall process governing mass transfer is not the rate at which interphase mass transfer occurs within the source. Rather, it is the advective-dispersive transport of dissolved chemical away from the DNAPL subzone that is the primary process limiting mass transfer rates.

On the basis of observed distribution of mass transfer rates, it is concluded that mass transfer will result in erosion of the DNAPL at the perimeter of the subzone. Reductions in DNAPL saturations within the DNAPL subzone will be minor. The validity of this observation is supported by laboratory measurements of trichloroethylene (TCE) saturations in a column subjected to continuous throughput of aqueous phase [*Imhoff et al.*, 1994]. These workers observed an active dissolution interval at the leading edge of a source ranging between 0.01 and 0.021 m. Beyond the active front, apparent TCE saturations remained constant through time.

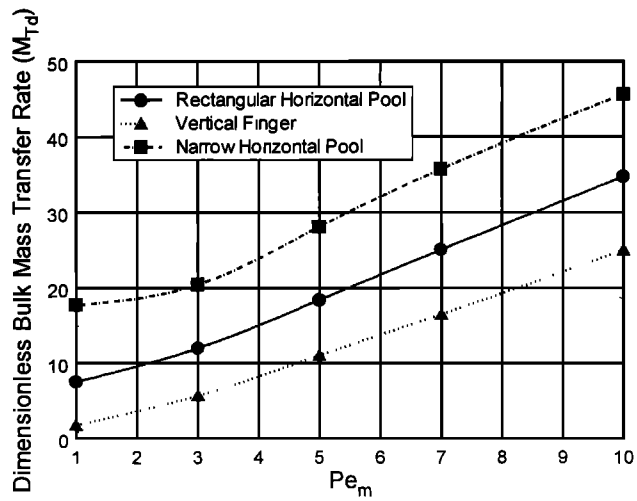

Figure 10. Sensitivity of dimensionless mass transfer to the macroscopic Peclet number.

An important implication of large mass transfer rates at the leading edge of a DNAPL subzone is that the overall rate of mass transfer is relatively insensitive to the length of the subzone. Shortening of a DNAPL subzone, either through natural dissolution or active remediation, has only small effects on bulk mass transfer rates and water quality downgradient of the subzone. This is because almost all of the mass transfer occurs at the leading edge of the source zone. Significant improvements in groundwater quality downgradient of the subzone will only occur when near-complete removal of the subzone is achieved.

7. Sensitivity of Mass Transfer Rates to Key Parameters

Variables controlling mass transfer rates are Sh_m, Pe_m, D_r, the dimensions of the DNAPL subzone, and the orientation of the subzone. Sensitivity to each of these factors is examined in Figures 9–11. In all three figures, consideration is given to a rectangular horizontal subzone oriented parallel to flow, a vertical finger oriented perpendicular to flow, and a narrow horizontal subzone oriented parallel to flow (see Figure 12). These shapes and orientations are based on the expected range of conditions that occur in DNAPL source zones.

In all cases, transport is three-dimensional, the flow field is

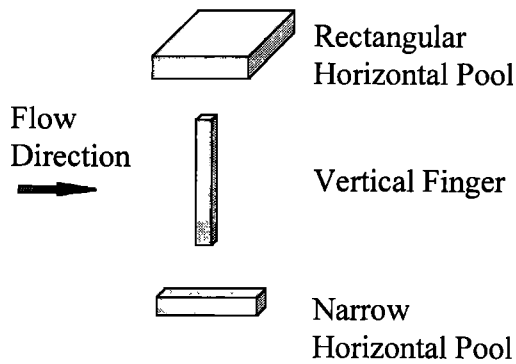

Figure 12. Geometry and orientation of DNAPL subzones considered.

Table 1. Characteristics of DNAPL Subzones

Subzone	Dimensionless Length (X)	Dimensionless Width (Y)	Dimensionless Height (Z)	Percent of Area Perpendicular to Flow	Dimensionless Volume
Rectangular horizontal subzone	1	1	0.1	4.4%	0.1
Vertical finger	1	1	10	31%	10
Narrow horizontal subzone	1	0.1	0.1	2.4%	0.01

uniform, and the DNAPL zones are subdivided into 48 subzones. The pattern of subdivision is similar to that shown in Figure 8 with the addition of four subdivisions in the Y dimension following the pattern used in the Z dimension. The dimensions of subzones were determined so that the total transfer rate ($\dot{M}_{Td}$) from each subzone was approximately equal. A different distribution of subzones was used for each set of conditions evaluated. This reflects the fact that the distribution of mass transfer rates is a function of the conditions evaluated. Further subdivision of the source was deemed unnecessary since it had no effect on $\dot{M}_{Td}$ as calculated for the entire subzone. Less subdivision resulted in lower estimates of mass transfer. As a worst case, use of a single subzone resulted in underestimation of mass transfer by 30%. Characteristics of the DNAPL subzones are listed in Table 1. Results presented in Figure 9–11 were calculated using (43) and (44).

Figure 9 is a plot of $\dot{M}_{Td}$ as a function of Sh_m for $D_r = 100$ and $Pe_m = 10$. The primary feature illustrated in Figure 9 is that bulk mass transfer from the source is a weak function of Sh_m. Increasing Sh_m by 5 orders of magnitude increases $\dot{M}_{Td}$ by factors ranging between 2 and 5 depending on the source geometry considered. For Sh_m values greater than 1×10^3, $\dot{M}_{vd}$ is practically independent of Sh_m. Similar results are observed for the plausible ranges of D_r and Pe_m.

Measured mass-transfer-rate coefficients (K_L) are of the order of 100 to 1000 day^{-1} [*Miller et al.*, 1990; *Imhoff et al.*, 1994]. Typical horizontal subzone lengths are probably greater than 0.1 m, and typical field groundwater velocities are in the range of 0.1–0.01 m d^{-1}. These typical conditions correspond to a range of Sh_m of 1×10^3 to 1×10^5. Therefore Figure 9 indicates that $\dot{M}_{vd}$ from subzones with L greater than 0.1 m are insensitive to Sh_m. In the case of DNAPL fingers and small horizontal subzones, L values as small as 0.01 m are plausible. For this condition a lower bound for Sh_m is 10. Even in this range, mass transfer rates remain a weak function of Sh_m.

Since Sh_m is a function of DNAPL saturation [e.g., *Hunt et al.*, 1988; *Powers et al.*, 1992], it follows that mass transfer rates will be largely insensitive to DNAPL saturations within subzones. This is a critical conclusion because it suggests that remedial technologies that primarily reduce DNAPL saturation in subzones will have a minor effect on near-term mass transfer rates from DNAPL source zones.

MASST does not account for reduced flow through DNAPL zones due to relative permeability effects. This requires consideration of when the assumption of uniform flow is reasonable. First, the uniform flow assumption is reasonable where DNAPL saturations are low (e.g., in vertical fingers that have drained to residual saturations). Second, the error introduced by ignoring relative permeability effects is small where the height (z dimension) of a subzone is small relative to its length (x dimension) (e.g., thin horizontal lenses and pools). As the height of a DNAPL zone goes to zero, mass transfer due to flow through the DNAPL zone and the significance of relative permeability effects go to zero. Reflecting on drained vertical fingers and thin horizontal lenses/pools as the primary features in DNAPL source zones, the assumption of uniform flow through DNAPL subzones should not introduce large errors in our analysis. Greater attention to mass transfer due to flow through subzones is presented in a subsequent section.

A convenient consequence of the insensitivity of $\dot{M}_{Td}$ to Sh_m is that precise estimates of Sh_m are not necessary to develop reasonable estimates of bulk mass transfer. The net effect of varying Sh_m is to modify the distribution of mass transfer rates within a horizontal subzone (as shown in Figure 8) but not the overall bulk mass transfer rate from the horizontal subzone. As an example, decreasing Sh_m in the case of Figure 8 leads to lower rates of mass transfer along the edges of the subzones but larger rates of mass transfer in the interior. Essentially no net change in the overall rate of mass transfer is observed upon reducing Sh_m. This conclusion contrasts with results from one-dimensional laboratory studies that have emphasized the importance of determining a pore-scale Sherwood number [*Miller et al.*, 1990; *Parker et al.*, 1991; *Powers et al.*, 1994; *Geller and Hunt*, 1993; *Imhoff et al.*, 1994; *Powers et al.*, 1994]. The explanation of this difference is that mass transfer from large DNAPL subzones ($L > 0.1$ m) is constrained more by the rates at which mass is transported away from subzone than by rates of interphase mass transfer within the subzone. The above referenced experiments were not designed to observe any limitation imposed on dissolution rates imposed by the rates at which dissolved mass is transported away from the subzones.

Attention is now turned to an analysis of $\dot{M}_{Td}$ as a function of Pe_m (see Figure 12). For these calculations, Sh_m and D_r are held constant at 1×10^5 and 1×10^2, respectively. The selected range of Pe_m values is based on typical conditions in granular porous media and seepage velocities of the order 0.01 to 1 m d^{-1}. Data in Figure 10 indicate that a tenfold increase in Pe_m results in a fourfold increase in $\dot{M}_{Td}$. Recognizing that D_L occurs in the denominator of both $\dot{M}_{Td}$ and Pe_m. Figure 11 also illustrates the dependence of dimensional mass transfer rate $\dot{M}_v$ ($M\ T^{-1}\ L^{-3}$) on V_w for DNAPL zones of fixed length. Thus a factor of 10 increase in flow field velocities only increases $\dot{M}_v$ by a factor of 4. In part, this provides an explanation for limited effectiveness of pump and treat as a remedial technology for DNAPL zones.

Finally, attention is turned to $\dot{M}_{Td}$ as a function of D_r (see Figure 11). For these calculations, Sh_m and Pe_m are held constant at 1×10^5 and 10, respectively. In systems where mechanical dispersion dominates molecular diffusion ($V_w > 0.01$ m d^{-1}), D_r can be estimated as the ratio of α_L and α_T. A likely range for D_r is 100–1000. Because longitudinal transport is dominated by advection, bulk mass transfer from a DNAPL source is only a weak function of D_L. Consequently, data posted in Figure 11 are primarily an analysis of the sensitivity to transverse hydrodynamic dispersion. Small values of

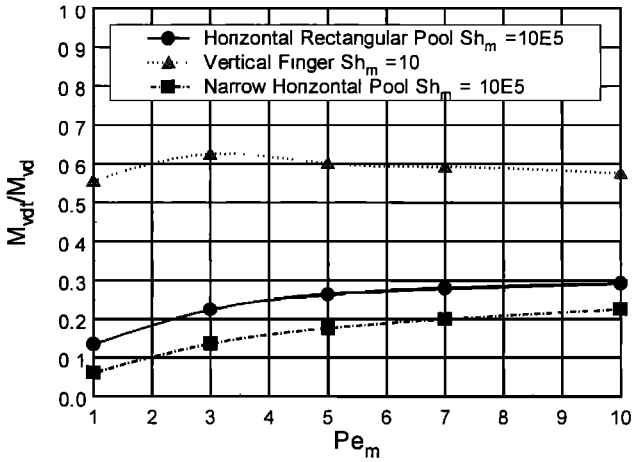

Figure 13. Fraction of total mass transfer attributable to advective transport through subzones.

D_r reflect large values of D_T. The effect of smaller values of D_r is an increase in the rate at which mass moves away from the source in the transverse direction and, consequently, larger rates of bulk mass transfer.

Also shown in Figure 11 is the sensitivity of $\dot{M}_{Td}$ to D_r for different geometries and orientations of the subzone. In the case of the vertical finger, $\dot{M}_{Td}$ is insensitive to variation in D_r. This is because mass transfer from the source is largely attributable to flow through the source, as opposed to transverse dispersion from the surfaces of the source. Progressively greater sensitivity to D_r is observed as the fraction of total source surface area on the face of the subzone influent to flow is decreased. This can be seen by considering the rectangular and narrow horizontal subzones with 4.4% and 2.4% of total surface area on the influent face of the subzone, respectively. These subzones, with smaller fractions of total surface area on the influent face of the subzone, show greater dependence on D_r and, correspondingly, D_T. To some degree the insensitivity of the vertical finger to D_r can be attributed to the large relative dimensionless volume of the vertical finger source (see Table 1). Nevertheless, results in Figure 11 illustrate that the fraction of mass transfer resulting from flow through a subzone, as opposed to that which results from transverse dispersion along the surfaces of a subzone, is a function of subzone geometry and orientation to flow.

8. Mass Transfer Attributable to Flow Through DNAPL Subzones

The sensitivity to subzone orientation and geometry illustrated in Figure 11 raises the issue of what fraction of total mass transfer is attributable to flow through a subzone. The importance of this issue is further increased by the fact that MASST assumes a uniform flow field throughout the solution domain. In actuality, owing to relative permeability effects, the presence of DNAPL in the subzone effects flow through and about the subzone [e.g., *Powers et al.*, 1998]. The following explores the significance of the assumption of uniform flow within and adjacent to a DNAPL subzone.

As a first step, an estimate of mass transfer due to flow through the subzone is developed. Considering a single DNAPL subzone, the mass transfer rate due to flow through a subzone on a unit volume basis ($\dot{M}_{vt}$) can be estimated as

$$\dot{M}_{vt} = \frac{\overline{C_e} V_w WH\phi}{LWH} = \frac{\overline{C_e} V_w \phi}{L} \tag{47}$$

where W is the length of the subzone in the y dimension, H is the length of the subzone in the z dimension, and $\overline{C_e}$ is the average effluent concentration from the subzone. Substitution of the mass transfer rate expressed by (47) for $\dot{M}_T$ in (46) results in

$$\dot{M}_{vdt} = \frac{\overline{C_e} V_w \phi}{L} L^2/D_f C_s \phi = Pe_m \bar{C}_{ne}. \tag{48}$$

Equation (48) illustrates that the dimensionless mass transfer rate per unit volume due to flow through the subzone, $\dot{M}_{vdt}$, can be estimated as the product of Pe_m and the normalized mean concentration on the downstream face of the subzone, $\bar{C}_{ne}$.

As a second step, the fraction of mass transfer per unit volume attributable to flow through a subzone is expressed as a fraction of the total mass transfer rate per unit volume, $\dot{M}_{vdt}/\dot{M}_{vd}$. Note that $\dot{M}_{vd}$ is the dimensionless mass transfer rate per unit volume of the entire source.

Figure 13 plots the fraction $\dot{M}_{vdt}/\dot{M}_{vd}$ as a function of Pe_m. A value of 1×10^5 is assigned to Sh_m for horizontal subzones. This reflects typical field conditions and a subzone length of 1 m. For the vertical finger a Sh_m value of 10 is considered. This reflects typical field conditions and a finger length in the direction of flow of 0.01 m. In the case of horizontal subzones, 5–30% of the total mass transfer is attributable to advective transport through the source. In the case of a finger perpendicular to flow, 55–60% of mass transfer is due to advective transport through the source. Where DNAPL saturations (S_n) are low (e.g., <0.1), the fraction of the total mass transfer due to flow through the subzones will be close to estimates of $\dot{M}_{vdt}/\dot{M}_{vd}$ presented in Figure 13. This is because the presence of low DNAPL saturations will have little effect on flow rates through the subzone. In the case of large DNAPL saturation, flow through the subzones will approach zero and the error associated with the uniform flow assumption will approach the fraction $\dot{M}_{vdt}/\dot{M}_{vd}$ shown in Figure 13.

9. Source Zones With Multiple DNAPL Subzones

Finally, consideration is given to a source zone containing multiple DNAPL subzones. Figure 14 is a cross section that depicts the distribution of normalized concentration surrounding five horizontal subzones. Parameters associated with each horizontal subzone are the same as those used for the single subzone presented in Figure 8. As observed in laboratory pool studies [*Whelan et al.*, 1994; *Pearce et al.*, 1994], steep concentration gradients exist above and below the subzones. Also shown in Figure 14 are $\dot{M}_{vd}$ values for the individual subzones. From the posted data it can be seen that subzones A, C, and E all have essentially the same mass transfer rates. Mass transfer from these subzones is independent of mass transfer from other portions of the source zone. On the other hand, mass transfer rates from subzones B and D are reduced due to interference from other subzones. Mass transfer from these subzones is dependent on mass transfer occurring at other locations in the source zone. In the case of B, immediately downgradient of A, the mass transfer rate is reduced by a factor of 4. In the case of D, slightly offset from C, the reduction in the rate of mass transfer is slight. These results illustrate

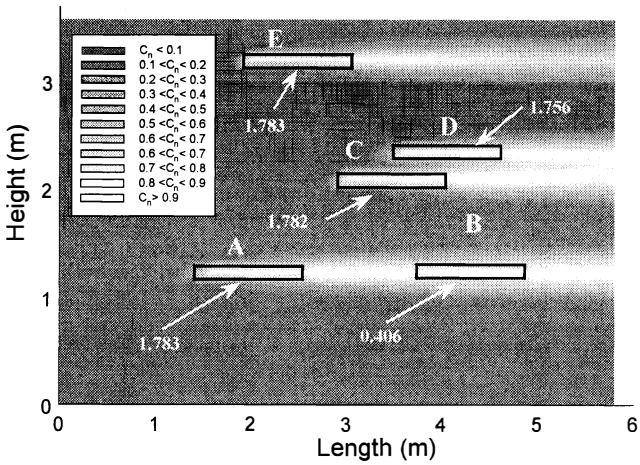

Figure 14. Normalized concentration distribution and mass transfer rates in a multiple subzone source.

that the architecture of subzones within a source zone can play an important role in constraining bulk mass transfer from source zones. In addition, Figure 14 leads to the observation that removing subzones that are either affected by upgradient subzones or interfering with downgradient subzone may have little effect on bulk mass transfer rates from DNAPL source zones.

10. Summary

MASST represents a fully three-dimensional analysis of mass transfer from DNAPL subzones that simultaneously accounts for the rate-limiting aspects of interphase mass transfer and advective-dispersive transport. Through this development it is shown that the primary process limiting mass transfer rates is advective-dispersive transport in the aqueous phase and not the internal rate of dissolution characterized by the mass transfer rate coefficient. This leads to the complementary observations that (1) mass transfer rates are largely independent of DNAPL saturations within DNAPL subzones and (2) remediations that reduce DNAPL saturations will have little effect on near-term groundwater quality.

MASST also demonstrates that mass transfer occurs primarily at the leading edges of subzones. Mass transfer through the remainder of the source is inhibited by interference from the upstream portion of the subzone. As a result, mass transfer rates and the duration of mass transfer from individual subzones is a function of their geometry and orientation to flow. Long DNAPL pools have low rates of mass transfer per unit volume and consequently persist for long periods of time. Conversely, thin DNAPL fingers have large relative rates of mass transfer per unit volume and persist for relatively short periods of time. Larger rates of mass transfer at the leading edges of subzones also lead to the observation that the dimensions of DNAPL subzones will decrease over time, while DNAPL saturations within subzones change only slightly. Unfortunately, due to locally larger rates of mass transfer at the leading edges of subzones, near-complete removal of DNAPL subzones is likely required to achieve meaningful improvements in groundwater quality.

Considering complex sets of DNAPL subzones, it is shown that interferences also can exist between individual subzones within the overall source zone. Manifestations of interferences between subzones are reduced rates of mass transfer per volume of DNAPL subzones and increased source longevity. As a result, remediation that removes subzones that are dependent or activates mass transfer from dependent subzones will have little effect on near-term groundwater quality.

A key feature of the MASST procedure is that it is computationally efficient. Within the context of uniform flow conditions, this makes possible routine analysis of mass transfer from complex DNAPL source zones. The principal limitation of the approach is that real conditions are far more complex than those that can be accounted for using analytical solutions that rely on uniform flow fields. Nevertheless, we feel that MASST effectively describes the principal factors governing mass transfer from DNAPLs in porous media and that the insights gained have applicability to real DNAPL source zones.

At present, techniques presented in this paper are being extended to account for mass transfer from DNAPL source zones through time. This allows analysis of both the near- and long-term benefits of DNAPL source-zone remediation. Also, the techniques are being expanded to account for multicomponent DNAPL and reactive transport.

Acknowledgments. The authors gratefully acknowledge the financial support of the Boeing Company through the Contaminant Hydrology Fund. This fund was established at Colorado State University, as part of the Solvents-in-Groundwater Research Consortium, University of Waterloo, Waterloo, Ontario, Canada.

References

Anderson, M. R., R. L. Johnson, and J. F. Pankow, Dissolution of dense chlorinated solvents into groundwater, 3, Modeling of contaminant plumes from fingers and pools of solvent, *Environ. Sci. Technol.*, *26*, 901–908, 1992.

Bear, J., *Dynamics of Fluids in Porous Media*, Elsevier Sci., New York, 1972.

Bird, R. B., W. E. Stewart, and E. N. Lightfoot, *Transport Phenomena*, John Wiley, New York, 1960.

Cohen, R. M., and J. W. Mercer, *DNAPL Site Evaluation*, CRC Press, Boca Raton, Fla., 1993.

Feenstra, S., and N. Guiger, Dissolution of dense nonaqueous phase liquids (DNAPLs) in the subsurface, in *Dense Chlorinated Solvents and Other DNAPLs in Groundwater*, edited by J. F. Pankow and J. A. Cherry, chap. 7, pp. 203–232, Waterloo Press, Portland, Oreg., 1996.

Feenstra, S., J. A. Cherry, and B. L. Parker, Conceptual models for the behavior of dense nonaqueous phase liquids (DNAPLs) in the subsurface, in *Dense Chlorinated Solvents and Other DNAPLs in Groundwater*, edited by J. F. Pankow and J. A. Cherry, chap. 2, pp. 53–88, Waterloo Press, Portland, Oreg., 1996.

Geller, J. T., and J. R. Hunt, Mass transfer from nonaqueous phase organic liquids in water-saturated porous media, *Water Resour. Res.*, *29*(4), 833–845, 1993.

Hunt, B., Dispersion sources in uniform groundwater flow, *J. Hydraul. Div. Am. Soc. Civ. Eng.*, *104*(HY1), 75–85, Jan. 1960.

Hunt, J. R., N. Sitar, and K. S. Udell, Nonaqueous phase liquid transport and cleanup, 1, Analysis of mechanisms, *Water Resour. Res.*, *24*(8), 1247–1258, 1988.

Imhoff, P. T., P. R. Jaffe, and G. F. Pinder, An experimental study of complete dissolution of a nonaqueous phase liquid in saturated porous media, *Water Resour. Res.*, *30*(2), 307–320, 1994.

Johnson,R. L., and J. F. Pankow, Dissolution of dense chlorinated solvents into groundwater, 2, Source functions for pools of solvent, *Environ. Sci. Technol.*, *26*, 869–901, 1992.

Kueper, B. H., and E. O. Frind, Two-phase flow in heterogeneous porous media, 1, Model development, *Water Resour. Res.*, *27*(6), 1049–1057, 1991a.

Kueper, B. H., and E. O. Frind, Two-phase flow in heterogeneous porous media, 2, Model application, *Water Resour. Res.*, *27*(6), 1058–1070, 1991b.

Kueper, B. H., and J. I. Gerhard, Variability of point source infiltration

rates for two-phase flow in heterogeneous porous media, *Water Resour. Res.*, *31*(12), 2971–2980, 1995.

Kueper, B. H., W. Abbot, and G. Farguhar, Experimental observations of multiphase flow in heterogeneous porous media, *J. Contam. Hydrol.*, *5*, 83–95, 1989.

Kueper, B. H., D. Redman, R. C. Starr, S. Reistma, and M. Mah, A field experiment to study the behavior of tetrachloroethylene below the watertable: Spatial distribution of residual and pooled DNAPL, *J. Ground Water*, *31*, 756–766, 1993.

MathSoft, Inc., *Mathcad User's Guide—Mathcad 7.0*, Cambridge, Mass., 1997.

Mayer, A. S., and C. T. Miller, The influence of mass transfer characteristics and porous media heterogeneity on nonaqueous phase dissolution, *Water Resour. Res.*, *32*(6), 1551–1567, 1996.

Miller, C. T., M. M. Poirier-McNeill, and A. S. Mayer, Dissolution of trapped nonaqueous phase liquids: Mass transfer characteristics, *Water Resour. Res.*, *26*(11), 2783–2796, 1990.

Parker, B. L., and D. B. McWhorter, Diffusive disappearance of immiscible phase organic liquids in fractured media: Finite matrix blocks and implications for remediation, paper presented at the International Symposium on Transport and Reactive Processes in Aquifers, Eidg. Tech. Hochsch., Zurich, Switzerland, April 11–15, 1994.

Parker, B. L., J. A. Cherry, and R. W. Gillham, The effects of molecular diffusion on DNAPL behavior in fractured porous media, in *Dense Chlorinated Solvents and Other DNAPLs in Groundwater*, edited by J. F. Pankow and J. A. Cherry, chap. 12, pp. 355–393, Waterloo Press, Portland, Oreg., 1996.

Parker, J. C., A. K. Katyal, J. J. Kaluaraachchi, R. J. Lenhard, T. J. Johnson, K. Jayaraman, K. Unlu, and J. L. Zhu, Modeling multiphase organic chemical transport in soils and ground water, *Rep. EPA/600/2-91/042*, U.S. Environ. Prot. Agency, Washington, D. C., 1991.

Pearce, A. E., E. A. Voudrias, and M. P. Whelan, Dissolution of TCE and TCA pools in saturated subsurface systems, *J. Environ. Eng.*, *120*(5), 1191–1206, 1994.

Poulson, M. M., and B. H. Kueper, A field experiment to study the behavior of tetrachloroethylene in unsaturated porous media, *Environ. Sci. Technol.*, *26*, 889–895, 1992.

Powers, S. E., C. O. Loureiro, L. M. Abriola, and W. J. Weber Jr., Theoretical study of the significance of nonequilibrium dissolution of nonaqueous phase liquids in subsurface systems, *Water Resour. Res.*, *27*(4), 463–477, 1991.

Powers, S. E., L. M. Abriola, and W. Weber Jr., An experimental investigation of nonaqueous phase liquid dissolution in saturated subsurface systems: Steady state mass transfer rates, *Water Resour. Res.*, *28*(10), 2691–2705, 1992.

Powers, S. E., L. M. Abriola, and W. Weber Jr., An experimental investigation of nonaqueous phase liquid dissolution in saturated subsurface systems: Transient mass transfer rates, *Water Resour. Res.*, *30*(2), 321–332, 1994.

Powers, S. E., I. M. Nambi, and G. W. Curry Jr., Nonaqueous phase liquid dissolution in heterogeneous systems: Mechanisms and a local equilibrium modeling approach, *Water Resour. Res.*, *34*(12), 3293–3302, 1998.

Sale, T. C., Interphase mass transfer from single component DNAPLs, Ph.D. dissertation, Colo. State Univ., Fort Collins, 1998.

Schwille, F., *Dense Chlorinated Solvents in Porous and Fractured Media*, translated by J. F. Pankow, Lewis, Boca Raton, Fla., 1988.

Strack, D. L., *Groundwater Mechanics*, Prentice-Hall, Englewood Cliffs, N. J., 1989.

U.S. Environmental Protection Agency, Guidance for evaluating the technical impracticability of groundwater restoration interim final report, *Publ. 9234.2-25*, *EPA/540/R/93/080*, Off. of Solid Waste and Emergency Response, Washington, D. C., 1993.

van Genuchten, M. T., and W. J. Alves, Analytical solution of the one-dimensional convective-dispersive solute transport equation, U.S. Dep. of Agric., Washington, D. C., 1982.

Voudrias, E. A., and M. F. Yeh, Dissolution of a toluene pool under constant and variable hydraulic gradients with implications for aquifer restoration, *J. Ground Water*, *32*(2), 305–311, 1994.

Whelan, M. P., A. Evangelos, and A. Pearce, DNAPL pool dissolution in saturated porous media: Procedures development and preliminary results, *J. Contam. Hydrol.*, *15*, 223–237, 1994.

D. B. McWhorter and T. C. Sale, Department of Chemical and Bioresource Engineering, Colorado State University, Fort Collins, CO 80523-1370. (dave@engr.colostate.edu; tsale@lamar.colostate.edu)

(Received September 22, 1999; revised June 27, 2000; accepted August 2, 2000.)